A novel high-voltage light punch-through carrier stored trench bipolar transistor with buried p-layer*

Zhang Jin-Ping(张金平)†, Li Ze-Hong(李泽宏), Zhang Bo(张 波), and Li Zhao-Ji(李肇基)

State Key Laboratory of Electronic Thin Films and Integrated Devices, University of Electronic Science and Technology of China, Chengdu 610054, *China*

(Received 15 November 2011; revised manuscript received 2 March 2012)

A novel high-voltage light punch-through (LPT) carrier stored trench bipolar transistor (CSTBT) with buried p-layer (BP) is proposed in this paper. Since the negative charges in the BP layer modulate the bulk electric field distribution, the electric field peaks both at the junction of the p base/n-type carrier stored (N–CS) layer and the corners of the trench gates are reduced, and new electric field peaks appear at the junction of the BP layer/N^- drift region. As a result, the overall electric field in the N^- drift region is enhanced and the proposed structure improves the breakdown voltage (BV) significantly compared with the LPT CSTBT. Furthermore, the proposed structure breaks the limitation of the doping concentration of the N–CS layer (N_{N-CS}) to the BV, and hence a higher N_{N-CS} can be used for the proposed LPT BP–CSTBT structure and a lower on-state voltage drop ($V_{ce(sat)}$) can be obtained with almost constant BV. The results show that with a BP layer doping concentration of $N_{BP} = 7 \times 10^{15}$ cm^{-3}, a thickness of $L_{BP} = 2.5$ μm, and a width of $W_{BP} = 5$ μm, the BV of the proposed LPT BP–CSTBT increases from 1859 V to 1862 V, with N_{N-CS} increasing from 5×10^{15} cm^{-3} to 2.5×10^{16} cm^{-3}. However, with the same N^--drift region thickness of 150 μm and N_{N-CS}, the BV of the CSTBT decreases from 1598 V to 247 V. Meanwhile, the $V_{ce(sat)}$ of the proposed LPT BP–CSTBT structure decreases from 1.78 V to 1.45 V with N_{N-CS} increasing from 5×10^{15} cm^{-3} to 2.5×10^{16} cm^{-3}.

Keywords: carrier stored trench bipolar transistor, light punch-through, buried p-layer, breakdown voltage

PACS: 85.30.–z, 85.30.De, 85.30.Pq, 85.30.Tv **DOI:** 10.1088/1674-1056/21/6/068504

1. Introduction

Insulated gate bipolar transistors (IGBTs) are widely used in a variety of power switching cases, such as motor drivers, electric vehicles, and power supplies. They have already become one of the mainstream power devices in medium–high voltage applications, and their use is continuously expanding due to improvements in the device structure.[1−10] Over the last few years, IGBT performance has been significantly improved, owing to the appearance of trench gate, light punch-through (LPT), which is also referred to as soft punch-through or field stop, and carrier stored (CS) technology.[11−14] As an advanced IGBT structure, the carrier stored trench bipolar transistor (CSTBT) with LPT structure incorporates all these innovations and demonstrates excellent overall performance.[15−18] For the LPT CSTBT, a highly doped N-type CS (N–CS) layer is used to act as a hole barrier to improve the conductivity modulation in the drift region, hence realizing a low on-state voltage drop ($V_{ce(sat)}$) with high carrier density around the trench gates. The higher the N–CS layer doping, the lower the $V_{ce(sat)}$ that can be obtained. However, with the increase in N–CS layer doping, the breakdown voltage (BV) of the CSTBT is degraded severely compared with a conventional LPT trench IGBT (LPT C–TIGBT) due to enhanced electric field peaks at the junction of the P base/N–CS layer and the trench gate corners in the blocking state.

In this paper, for the first time, a high-voltage LPT CSTBT with a buried P-layer (BP) is proposed to address this main issue of the CSTBT structure. Although only the LPT-type CSTBT structure is discussed in the paper, the proposed structure can be easily applied to various CSTBT structures. In the next sections, the LPT BP–CSTBT, LPT CSTBT, and LPT C–TIGBT will be referred to as BP–CSTBT, CSTBT, and C–TIGBT, respectively.

*Project supported by the National Science and Technology Major Project of China (Grant No. 2011ZX02504-003) and the Fundamental Research Funds for the Central Universities, China (Grant No. ZYGX2011J024).

†Corresponding author. E-mail: jinpingzhang@uestc.edu.cn

© 2012 Chinese Physical Society and IOP Publishing Ltd

2. Device structure and operation

Figure 1 shows schematic cross sections of the IGBT structures: (a) proposed BP–CSTBT and (b) CSTBT. Compared with the case of CSTBT, an additional BP layer is embedded beneath the N–CS layer in the middle of the cell for the BP–CSTBT structure. For the CSTBT structure, a highly doped N–CS layer is placed at the bottom of the p-base layer to act as a hole barrier to improve the carrier density around

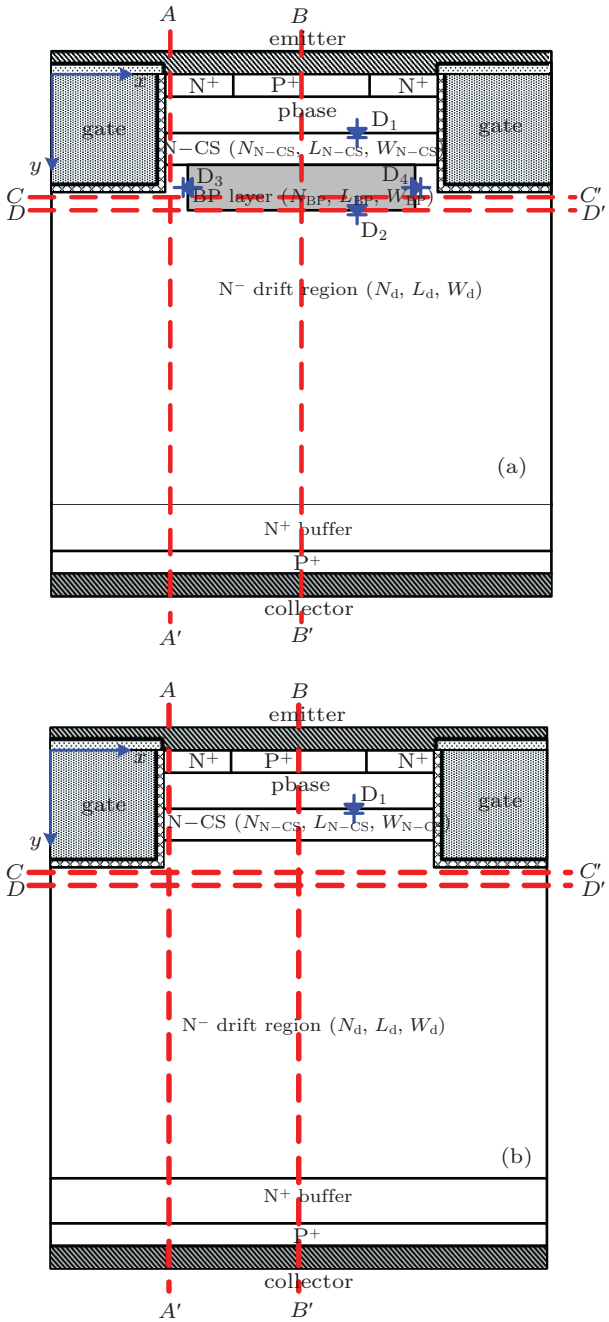


Fig. 1. (colour online) Schematic cross sections of the IGBT structures: (a) proposed BP–CSTBT, (b) CSTBT.

the trench gates. However, due to the higher doping concentration of the N–CS layer, the electric field peaks both at the D_1 junction and trench gate corners are enhanced in the forward blocking state. As a result, the BV of the CSTBT is degraded compared with the C–TIGBT. For the proposed BP–CSTBT structure, with the additional reverse biased D_2–D_4 junctions and negative charges introduced from the BP layer, the bulk electric field distribution is modulated. Therefore, the electric field peaks both at the D_1 junction and trench gate corners are reduced and new electric field peaks appear at the D_2, D_3, and D_4 junctions. The enhancement of the electric field at the D_2 junction increases the overall electric field in the N^- drift region. As a result, the BV of the BP–CSTBT is improved significantly compared with the C–TIGBT and CSTBT structures. In the next discussion, $N_{BP/N-CS/d}$, $L_{BP/N-CS/d}$, and $W_{BP/N-CS/d}$ are the doping concentration, thickness and width of the BP layer, N–CS layer and N^- drift region, respectively. To have a meaningful comparison, a CSTBT and C-IGBT with the same device parameters are also simulated. In the simulation, the electron and hole lifetimes are set to be 1 μs.

3. Results and discussion

Figure 2 shows the influences of the BP layer parameters on the BV of the BP–CSTBT structure: (a) the N_{BP} and (b) the L_{BP}. The parameters of the N–CS layer and N^- drift region used in the simulation are $N_{N-CS} = 1 \times 10^{16}$ cm^{-3}, $L_{N-CS} = 2$ μm, $W_{N-CS} = 6$ μm, $N_d = 6 \times 10^{13}$ cm^{-3}, $L_d = 150$ μm and $W_d = 8$ μm, respectively. It can be seen from Fig. 2(a) that with different values of L_{BP}, the BV of the BP–CSTBT structure increases quickly with the increase in N_{BP}, and when the BV achieves a maximum, it decreases slightly with the increase in N_{BP}. The larger the L_{BP}, the smaller the N_{BP} that is needed for the maximal BV. Figure 2(b) shows a similar relationship between the BV and the L_{BP} with different values of W_{BP} for the BP–CSTBT. The larger the W_{BP}, the smaller the L_{BP} is needed for the maximal BV. It can be observed that the BV of the proposed BP–CSTBT structure is affected by the total charge of the BP layer, and the key BP layer parameters should satisfy the following approximate condition to obtain a higher BV:

$$N_{BP} \times L_{BP} \times W_{BP} \geq N_d \times L_d \times W_d. \quad (1)$$

As long as the total charge of the BP layer is equal to or larger than the total charge of the N^- drift region, the effect of the positive charges of the N–CS layer on the BV can be shielded by the BP layer, and a near constant BV can be obtained for the proposed structure. This relationship between BV and BP layer parameters indicates that the BP–CSTBT has an excellent processing tolerance.

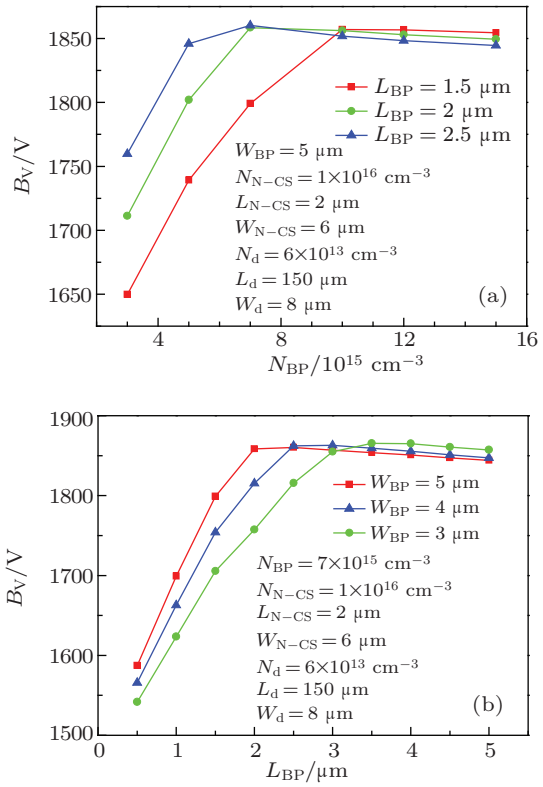


Fig. 2. (colour online) The influences of the BP layer parameters on the BV of the BP–CSTBT.

Forward blocking I–V characteristics for the BP–CSTBT structure are shown in Fig. 3. Based on the optimization result from Fig. 2, the device parameters used in the simulation are $N_{BP} = 7 \times 10^{15}$ cm^{-3}, $L_{BP} = 2.5$ μm, $W_{BP} = 5$ μm, $N_{N-CS} = 1 \times 10^{16}$ cm^{-3}, $L_{N-CS} = 2$ μm, $W_{N-CS} = 6$ μm, $N_d = 6 \times 10^{13}$ cm^{-3}, $L_d = 150$ μm, and $W_d = 8$ μm. For comparison, the results of the CSTBT and C–TIGBT with the same device parameters are also shown in Fig. 3. The simulation results show that the BV values of the BP–CSTBT, CSTBT, and C–TIGBT structures are 1860 V, 1437 V, and 1702 V, respectively. It can be seen that compared with the cases of the CSTBT and C–TIGBT, the BV of the BP–CSTBT is improved significantly. The negative influence of the highly doped N–CS layer on the BV of the CSTBT is addressed by the introduction of the BP layer. Figure 4 shows a comparison of the corresponding forward conduction I–V characteristics at $V_{ge} = 15$ V between the three structures. It can be seen that the BP–CSTBT structure retains the advantage of the CSTBT and has almost the same I–V characteristics. The values of the on-state voltage drop ($V_{ce(sat)}$) of the BP–CSTBT and CSTBT at collector current density $J_{ce} = 100$ A/cm^2 are 1.61 V and 1.53 V, respectively, which is significantly smaller than the 1.93 V of the C–TIGBT.

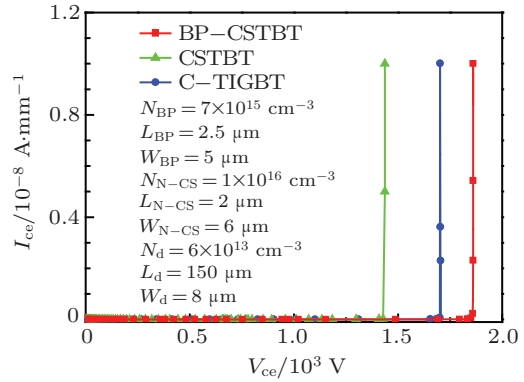


Fig. 3. (colour online) Forward blocking I–V characteristics.

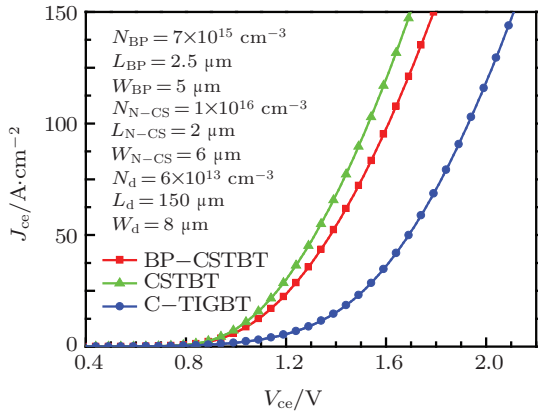


Fig. 4. (colour online) Forward conduction I–V characteristics.

Figure 5 shows the effects of the N_{N-CS} on the BV and $V_{ce(sat)}$ of the BP–CSTBT and CSTBT structures. For comparison, the BV and $V_{ce(sat)}$ of the C–TIGBT are also shown in the figure. It can be seen that the proposed structure breaks the limitation of the doping concentration of the N–CS layer (N_{N-CS}) to BV. The BV of the BP–CSTBT has almost no change with the increase in N_{N-CS}. However, the BV of the CSTBT is reduced significantly. The results show that with a BP layer doping concentration of $N_{BP} = 7 \times 10^{15}$ cm^{-3}, thickness of $L_{BP} = 2.5$ μm and width of $W_{BP} = 5$ μm, the BV of the proposed BP–CSTBT increases from 1859 V to 1862 V with the N_{N-CS} increasing from 5×10^{15} cm^{-3}

to 2.5×10^{16} cm^{-3}. However, with the same N$^-$ drift region thickness of 150 μm and $N_{\mathrm{N-CS}}$, the BV of the CSTBT decreases from 1598 V to 247 V. Even with the N–CS layer, the BV of the BP–CSTBT is larger than that of the C–TIGBT structure. The negative influence of the $N_{\mathrm{N-CS}}$ on the BV is shielded by the BP layer well for the BP–CSTBT structure. It can also be seen from Fig. 5 that the values of $V_{\mathrm{ce(sat)}}$ for both the CSTBT and BP–CSTBT decrease with the increase in $N_{\mathrm{N-CS}}$, and the BP–CSTBT structure even has a slightly larger reduction rate for the $V_{\mathrm{ce(sat)}}$. A higher $N_{\mathrm{N-CS}}$ can be used for the proposed BP–CSTBT structure and a lower $V_{\mathrm{ce(sat)}}$ can be obtained with almost constant BV. With the $N_{\mathrm{N-CS}}$ increasing from 5×10^{15} cm^{-3} to 2.5×10^{16} cm^{-3}, the $V_{\mathrm{ce(sat)}}$ decreases from 1.78 V to 1.45 V for the proposed BP–CSTBT structure.

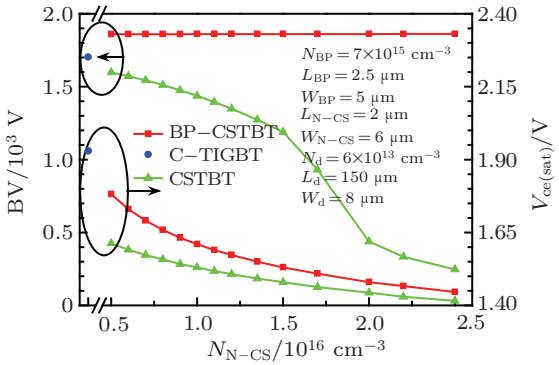


Fig. 5. (colour online) The effects of $N_{\mathrm{N-CS}}$ on BV and $V_{\mathrm{ce(sat)}}$.

Figure 6 shows the electric field distribution at breakdown for the structures with $N_{\mathrm{N-CS}} = 1\times10^{16}$ cm^{-3}: (a) AA' line, (b) BB' line, (c) CC' line, and (d) DD' line. The BV values of the BP–CSTBT, CSTBT and C–TIGBT structures are 1860 V, 1437 V, and 1702 V, respectively. It can be seen that the electric field distribution of the CSTBT has a higher peak value both at the trench gate corners and junction D_1 compared with that of C–TIGBT, which is induced by higher positive charge density from the N–CS layer. With vertical and lateral electric field modulation from the negative charges of the BP layer, the electric field peaks both at the trench gate corners and the D_1 junction are reduced and new electric field peaks appear at the D_2 junction for the proposed BP–CSTBT. With a higher electric field at the D_2 junction, the overall electric field in the N$^-$ drift region is enhanced, therefore, a higher blocking voltage is obtained for the proposed BP–CSTBT. Figure 7 shows the electric field distribution at breakdown for the structures with $N_{\mathrm{N-CS}} = 2 \times 10^{16}$ cm^{-3}: (a) AA' line, (b) BB' line,

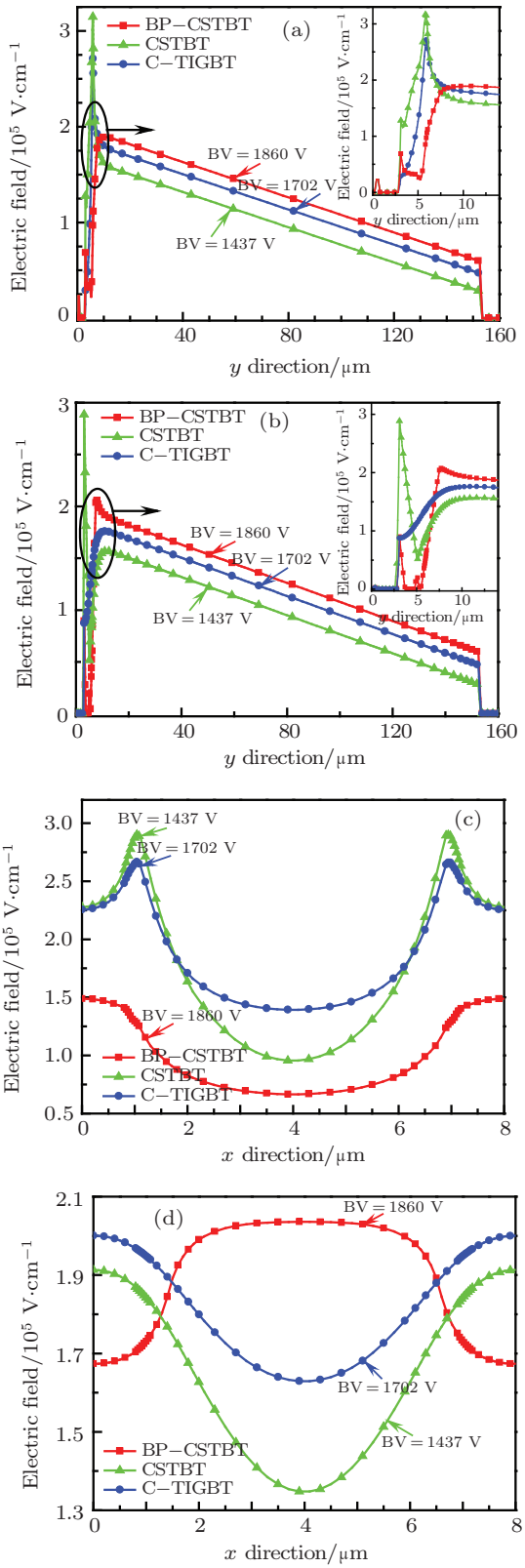


Fig. 6. (colour online) Electric field distribution at breakdown with $N_{\mathrm{N-CS}} = 1 \times 10^{16}$ cm^{-3}: (a) AA' line, (b) BB' line, (c) CC' line, and (d) DD' line. The parameters are taken as: $N_{\mathrm{BP}} = 7 \times 10^{15}$ cm^{-3}, $L_{\mathrm{BP}} = 2.5$ μm, $W_{\mathrm{BP}} = 5$ μm, $N_{\mathrm{N-CS}} = 1 \times 10^{16}$ cm^{-3}, $L_{\mathrm{N-CS}} = 2$ μm, $W_{\mathrm{N-CS}} = 6$ μm, $N_{\mathrm{d}} = 6 \times 10^{13}$ cm^{-3}, $L_{\mathrm{d}} = 150$ μm, and $W_{\mathrm{d}} = 8$ μm.

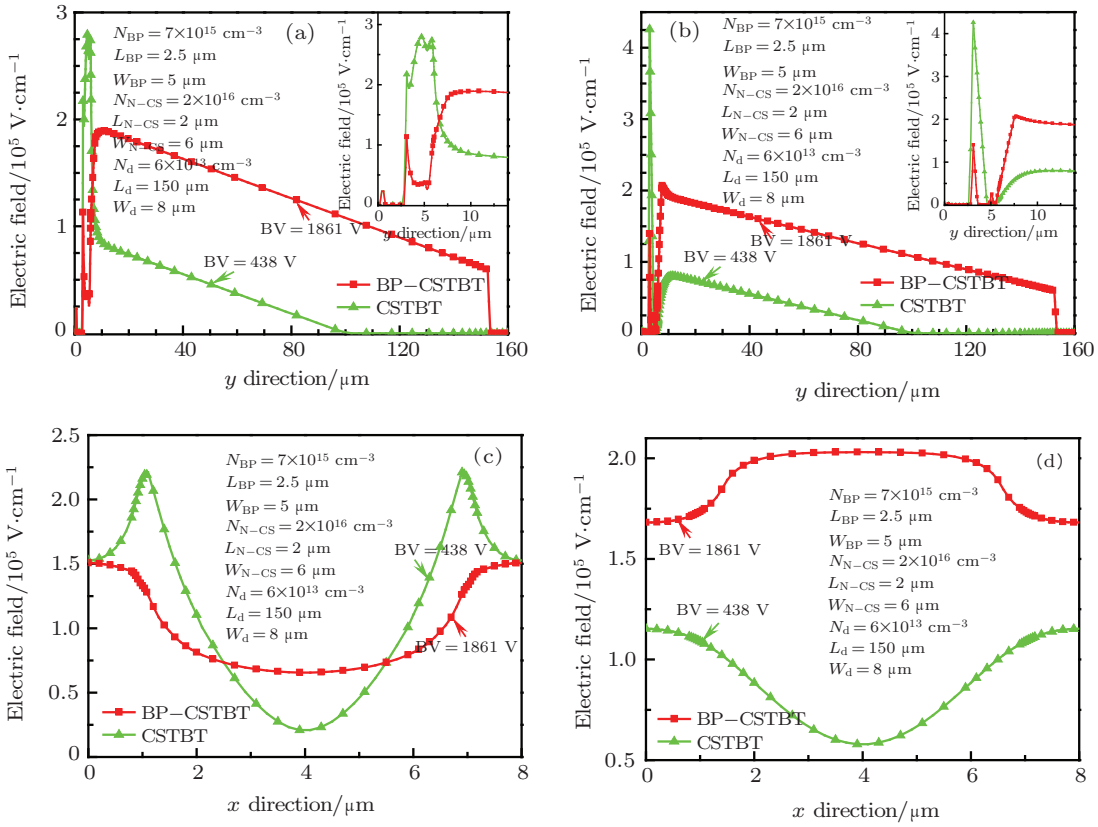


Fig. 7. (colour online) Electric field distribution at breakdown with $N_{N-CS} = 2 \times 10^{16}$ cm^{-3}: (a) AA' line, (b) BB' line, (c) CC' line, and (d) DD' line.

(c) CC' line, and (d) DD' line. The BV values of the BP–CSTBT and CSTBT structures are 1861 V and 438 V, respectively. It can be seen that with the N_{N-CS} increasing from 1×10^{16} cm^{-3} to 2×10^{16} cm^{-3}, the CSTBT is broken down even without depleting the N^- drift region due to the enhanced electric field peaks at the trench gate corners and D_1 junction. With electric field modulation from the negative charges of the BP layer, the electric field distribution at breakdown for the BP–CSTBT with $N_{N-CS} = 2 \times 10^{16}$ cm^{-3} is almost the same as that with $N_{N-CS} = 1\times10^{16}$ cm^{-3}. The negative influence of N_{N-CS} on the electric field is shielded by the BP layer well for the BP–CSTBT structure.

Figure 8 shows the influences of the N_{N-CS} on the BV of different voltage class BP–CSTBT and CSTBT devices. It can be seen that the curves of BV versus N_{N-CS} for the different voltage class devices have trends similar to those in Fig. 5. The BV of the BP–CSTBT remains almost unchanged with the increase in N_{N-CS}, however, the BV of the CSTBT decreases significantly. Based on this result, it can be concluded that the proposed structure is suitable for various high-voltage applications.

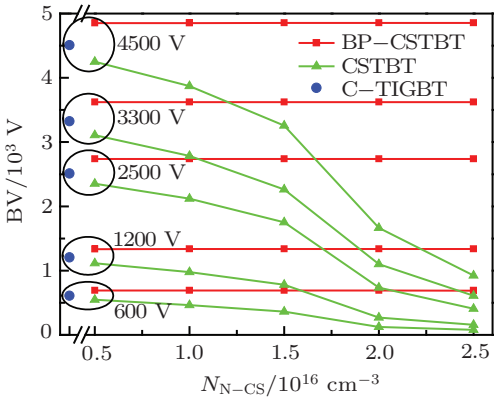


Fig. 8. (colour online) The influences of the N_{N-CS} on the BV of different voltage class devices.

4. Conclusion

A novel high-voltage LPT BP–CSTBT is proposed in this paper. The proposed structure improves the BV significantly compared with the LPT CSTBT due to the electric field modulation from the negative charges in the BP layer. Furthermore, the proposed structure breaks the limitation of the N_{N-CS}

to the BV, and hence a higher $N_{\mathrm{N-CS}}$ can be used for the proposed structure and a lower $V_{\mathrm{ce(sat)}}$ can be obtained with almost constant BV. The results show that with $N_{\mathrm{BP}} = 7 \times 10^{15}$ cm^{-3}, $L_{\mathrm{BP}} = 2.5$ μm and $W_{\mathrm{BP}} = 5$ μm, the BV of the proposed LPT BP–CSTBT increases from 1859 V to 1862 V, with $N_{\mathrm{N-CS}}$ increasing from 5×10^{15} cm^{-3} to 2.5×10^{16} cm^{-3}. However, with the same N^- drift region thickness of 150 μm and $N_{\mathrm{N-CS}}$, the BV of the CSTBT decreases from 1598 V to 247 V. Meanwhile, the $V_{\mathrm{ce(sat)}}$ of the proposed structure decreases from 1.78 V to 1.45 V with $N_{\mathrm{N-CS}}$ increasing from 5×10^{15} cm^{-3} to 2.5×10^{16} cm^{-3}.

References

[1] Li Z H, Qian M L and Zhang B 2009 *Proc. IEEE 21st International Symposium on Power Semiconductor Devices & IC's* June 14–18, 2009, Barcelona, Spain p. 124

[2] Antoniou M, Udrea F, Bauer F and Nistor I 2011 *IEEE Trans. Electron Dev.* **58** 769

[3] Vobecky J 2006 *Proc. 27th International Conference on Microelectronics*, May 16–19, 2010, NIŠ, Serbia p. 67

[4] Kopta A, Rahimo M, Eicher S and Schlapbach U 2006 *Proc. IEEE 18th International Symposium on Power Semiconductor Devices & IC's*, June 4–8, 2006, Naples, Italy p. 1

[5] Ranstad P and Nee H 2011 *IEEE Trans. Power Electronics* **26** 260

[6] Onozawa Y, Otsuki M, Iwamuro N, Miyashita S, Miyasaka T, Seki Y and Matsumoto T 2007 *IEEE Trans. Industry Appl.* **43** 513

[7] Zhang F, Shi L, Li C, Wang W, Yu W and Sun Xi 2006 *IEEE Trans. Plasma Sci.* **34** 1026

[8] Iwamoto H, Haruguchi H, Tomomatsu Y, Donlon J F and Motto E R 2002 *IEEE Trans. Industry Appl.* **38** 168

[9] Luo X R, Yao G L, Chen X, Wang Q, Ge R and Florin U 2011 *Chin. Phys.* B **20** 028501

[10] Hu S D, Wu L J, Zhou J L, Gan P, Zhang B and Li Z J 2012 *Chin. Phys.* B **21** 027101

[11] Laska T, Munzer M, Pfirsch F, Schaeffer C and Schmidt T 2000 *Proc. IEEE 12nd International Symposium on Power Semiconductor Devices & IC's* May 22–25, 2000, Toulouse, France p. 355

[12] Oyama K, Arai T, Saitou K, Masuda K and Mori M 2004 *Proc. IEEE 16th International Symposium on Power Semiconductor Devices & IC's*, May 24–27, 2004, Milan, Italy p. 111

[13] Mori M, Oyama K, Arai T, Sakano J, Nishimura Y, Masuda K, Saito K, Uchino Y and Homma H 2007 *IEEE Trans. Electron Dev.* **54** 1515

[14] Onozawa Y, Ozaki D, Nakano H, Yamazaki T and Fujishima N 2011 *Proc. IEEE 23th International Symposium on Power Semiconductor Devices & IC's*, May 23–26, 2011, San Diego, USA p. 52

[15] Takahashi T, Tomomatsu Y and Sato K 2008 *Proc. IEEE 20th International Symposium on Power Semiconductor Devices & IC's*, May 18–22, 2008, Florida, USA p. 72.

[16] Mori M, Oyama K, Kohno Y, Sakano J, Uruno J, Ishizaka K and Kawase D 2007 *IEEE Trans. Electron Dev.* **54** 2011

[17] Nakamura K, Sadamatsu K, Oya D, Shigeoka H and Hatade K 2010 *Proc. IEEE 22th International Symposium on Power Semiconductor Devices & IC's*, June 6–10, 2010, Hiroshima, Japan p. 387

[18] Haraguchi Y, Honda S, Nakata1 K, Narazaki A and Terasaki Y 2011 *Proc. IEEE 23th International Symposium on Power Semiconductor Devices & IC's*, May 23–26, 2011, San Diego, USA p. 68